eJSE International
Electronic Journal of Structural Engineering 16(1) 2016

# Steel beams strengthened with prestressed CFRP laminate: is there a need for laminate prestressing?

M.A. Gharib
*IBSF, Saudi Arabia*

W.H. Khushefati
*Assistant Professor, King Abdulaziz University, Saudi Arabia*

M.A. Khedr
*BC Hydro, Canada - Associate Professor, Dept. of Civil Eng., Faculty of Eng., Benha University*

E.Y. Sayed-Ahmed*
*Professor, Construction Engineering Dept., the American University in Cairo, Egypt*
*eysahmed@aucegypt.edu eysahned@gmail.com

ABSTRACT: Strengthening structural members using Carbon Fiber Reinforced Polymer (CFRP) laminate is an effective method to increase their strength. Prestressing the CRFP laminate prior to attaching them to a steel beam can delay the common premature debonding, which is the predominant failure mode when loading such composite elements in flexure. Following a previously published experimental investigation, this paper presents the results of a finite element simulation of steel I-beams strengthened with bonded and mechanically anchored prestressed CFRP laminate subjected to flexural loading. The numerical analysis adopts a Cohesive Zone Model (CZM) technique to simulate the separation between the CFRP laminate and the steel beam in order to model the debonding failure mode. The accuracy of the finite element model is verified by comparing its results to those of the previously published experimental investigation, which was carried out on steel I-beams strengthened with prestressed CFRP laminate in deferent configurations. The numerical model is then used to evaluate the effect of changing the level of the prestressing force on the strengthened beams performance. It is found that the CFRP prestressing enhances the yield and ultimate load carrying capacity of the beams and delays the typical premature debonding failure up to a certain level of laminate prestressing.

## 1 INTRODUCTION

Using of Carbon Fibre Reinforced Polymers (CFRP) strips in retrofitting and strengthening substandard steel structures [e.g. 1–4] is not as common as its usage for concrete and even masonry structures [e.g. 5–9]. For beams, this strengthening method usually consists of using CFRP laminate, which are typically attached to the beam's tension side using a layer of adhesive material [e.g. 5, 8]. The drawback of using such a procedure for retrofitting steel beams is the premature debonding failure of the laminate from the steel beam [3, 4, 10-13]. Some investigations introduced prestressing to the CFRP laminate as a solution to debonding issue and to fully utilize the strengthened section where prestressing may have a favourable effect of delaying this premature failure [10, 14, 15]. Several techniques can be used to apply the prestressing force to the CFRP but mechanical anchorages are needed to maintain the prestressing force applied to the CFRP laminate and ensure more ductile behaviour of the hybrid section [15, 16]. Many experimental investigations were also carried out to evaluate, understand and predict the behaviour of hybrid steel-CFRP sections [e.g. 17–23]. However, each of these studies were limited to a certain scope and a number of parameters and did not provide answers to concerns related to the premature debonding failure. A recent experimental investigation has been published by the authors [15], which showed that prestressing the CFRP laminate and using end anchorages could overcome the shortcoming associated with the debonding premature failure mode.

On another frontier related to numerical analyses, finite element modelling is considered as a good approach to predict the performance of structures and structural elements. Some numerical investigation dealt with the CFRP laminate debonding using smeared damage concept [e.g. 24] which considers the cracked solid to be a continuum and describes the cracking propagation in terms of degradation of the material constitutive model. However, the use of this method does not fit the nature of debonding and/or delamination process. Discrete damage approach [25–28] may reflect the final damage state more closely: it models the crack directly in terms of traction-separation instead of stress-strain relationship via interface elements that separate the two discrete elements.

One of the most widely discrete damage models used for the analysis of debonding mechanisms is the cohesive zone modelling (CZM) approach, which bridges the gap between the stress and energy based approaches [27]. This approach assumes that the stress transfer capacity between the two separating faces after separation is not lost completely at damage initiation, but rather is a progressive event governed by progressive stiffness reduction of the interface between the two separating faces. Thus, it is a suitable method to model delamination of layered composites, and to describe the macroscopic constitutive behaviour of thin adhesive layer. In a CZM model, the interfacial normal and tangential stresses are non-linearly related to the normal (mode-I) and the tangential (mode-II) relative displacements across the interface [28]. As the cohesive interface gradually separates, the magnitude of the interfacial stresses at first increases, reaches its maximum level, and then decreases with increasing separation, until it approaches zero. The main advantage of this approach is the implementation of the crack nucleation and growth mechanisms in the stress analysis procedure.

As such, in this paper, a finite element model of steel beams subject to flexure and strengthened with prestressed CFRP with end mechanical anchorages is presented. The model adopts the CZM technique for simulating the CFRP debonding from the steel beam. The results obtained from the numerical analyses are first verified using the outcomes of an experimental investigation, which was previously performed and published by the authors [15]. The experimental investigation was carried out on steel beams to investigate the feasibility and effectiveness of prestressing the CFRP laminate on this strengthening technique. The numerical model is then adopted to predict the behaviour of the hybrid steel-CFRP section when changing the level of prestressing force applied to the CFRP laminate.

## 2 THE EXPERIMENTAL INVESTIGATION

Full details of the experimental investigation are given elsewhere [15] with only a brief outlines of this investigation presented herein. Description of four of the tested beams are given in Table 1.

Table 1. Tested beams details.

| Beam | CFRP laminate dimension | End anchorage | Prestressing force (kN) |
|---|---|---|---|
| CB1 | No | No | No |
| CB2 | 100 × 1.2mm | No | No |
| B3-25-AN | 100 × 1.2mm | Yes | 25 |
| B4-45-AN | 100 × 1.2mm | Yes | 45 |

All the beams have a W6×20 cross-section, and a total length of 2900 mm. Steel beams CB1, CB2 and B3 have yield strength of 390 MPa, while beam B4 has a yield strength of 350 MPa. Beam CB1 is the control beam with no CFRP strengthening. Beam CB2 is strengthened with bonded CFRP with no prestressing. Beams B3 and B4 are strengthened with prestressed CFRP: the prestressing force in the CFRP laminate were 25 kN and 45 kN, respectively. Both beams (Beams B3 and B4) have end mechanical anchorages for the prestressed CFRP laminate. Figure 1 shows a typical cross section of these strengthened steel beams at the end anchorage zone.

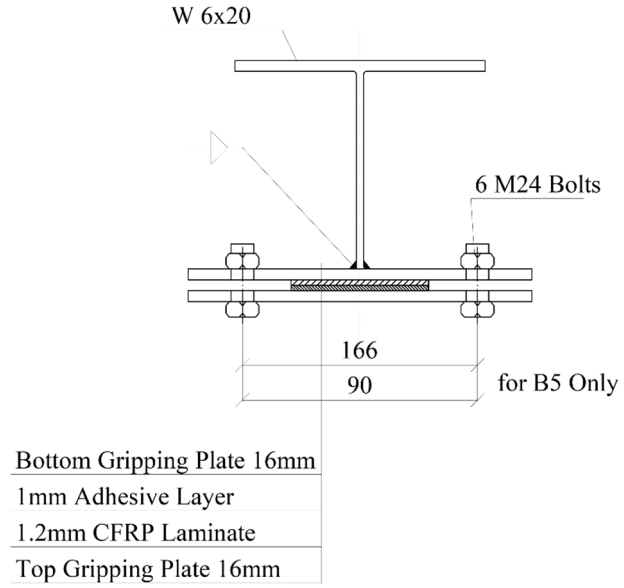


Figure 1. Strengthened steel beam's cross-section at the location of the gripping plates (Beams B3 and B4).

The mechanical properties of the steel beam, CFRP and adhesive were obtained from material testing and manufacture data sheet. These are summarized in Tables 2–4. All the CFRP laminate adopted in strengthening were 100 mm wide and 1.2 mm thick.

Table 2. Mechanical properties of the steel beams.

| Beam | Yield stress (MPa) | Tensile strength (MPa) |
|---|---|---|
| CB1 | 390 | 560 |
| CB2 | 390 | 560 |
| B3-25-AN | 390 | 560 |
| B4-45-AN | 350 | 520 |

Table 3. Properties of the CFRP laminate.

| Mechanical properties | Value (MPa) |
|---|---|
| Tensile modulus | 165,000 |
| Tensile strength | 3,100 |

Table 4. Properties of the epoxy adhesive.

| Mechanical properties | Value (MPa) |
|---|---|
| Tensile strength | 24.8 |
| Compressive strength | 61 |
| Shear strength | 24.8 |
| Bond strength | 18 |
| Tensile modulus | 4,400 |

All beams were tested in 4–points loading with a simply supported ends as shown in Figure 2. Along with Figure 1, Figure 2 schematically shows the end anchorage zone for the prestressed FRP laminate. Full details of the prestressing technique and the mechanical anchorage are given elsewhere [15]. The load was applied in prescribed increments to the beam using a universal testing machine. As previously concluded [15], prestressing the CFRP laminate generally reduced the deflection and delayed the premature debonding failure. Some of the results of the experimental investigation are summarized in Table 5.

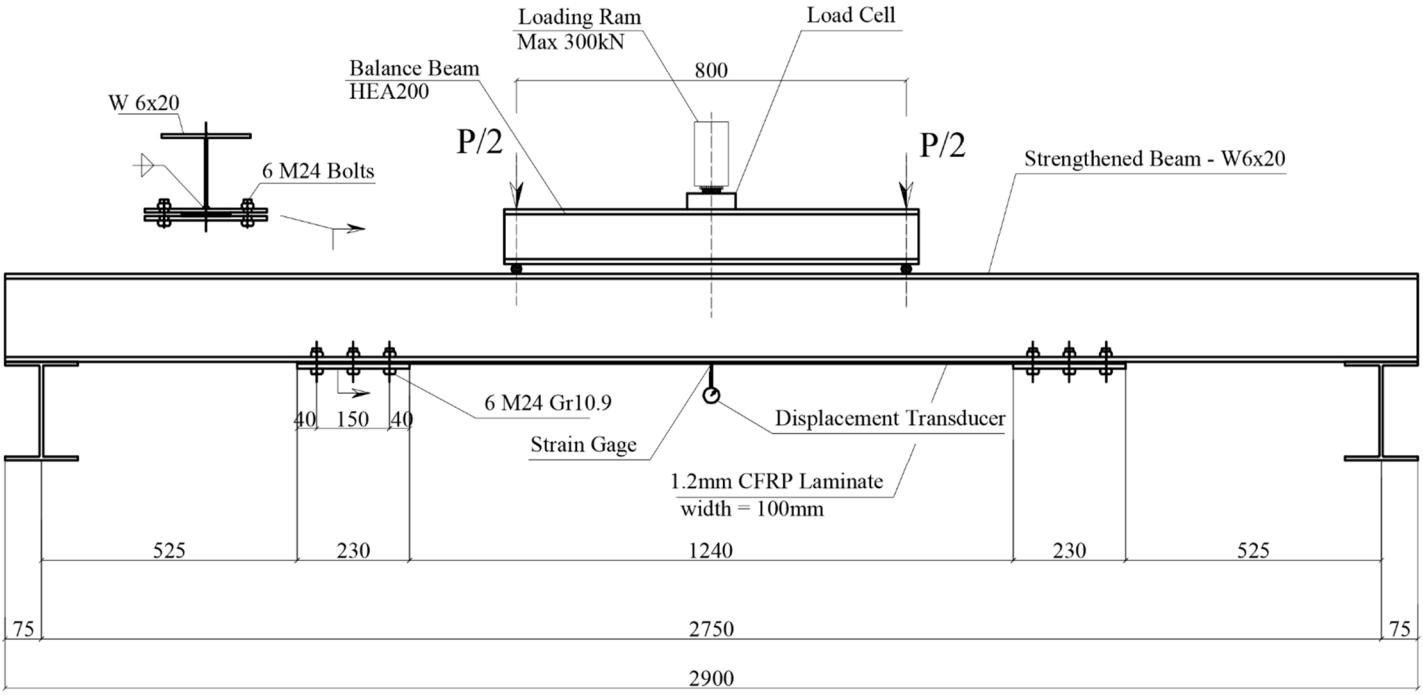


Figure 2. Test setup for a typical strengthened steel beam with CFRP prestressed laminate [15].

Table 5. Results of the experimental investigation performed on steel beams strengthened with CFRP laminate.

| Beam No. | CFRP jacking strain (με) | Yield Load $P_y$ (kN) | CFRP debonding load | | CFRP rupture load | | CFRP failure |
|---|---|---|---|---|---|---|---|
| | | | $P_{de}$ (kN) | Associated strain (με) | $P_{fru}$ (kN) | Associated strain (με) | |
| CB1 | – | 172.7 | N/A | N/A | N/A | N/A | N/A |
| CB2 | – | 174.8 | 193.2 | 5290 | no rupture | no rupture | debonding |
| B3-25-AN | 3140 | 194.6 | 204.5 | 3953 | 199.7 | 4435 | rupture |
| B4-45-AN | 3984 | 166.3 | 182.7 | 5725 | 190.5 | 9601 | rupture |

## 3 THE NUMERICAL MODEL

### 3.1 *The Finite element model*

The finite element program ANSYS® is used for pre-processing and building the model, solution of the model equations and post-processing the results. A three-dimension finite element model is developed accounting for both the geometric and the material nonlinear behaviour of the hybrid steel-CFRP beam. Newton-Raphson equilibrium is used for updating the model stiffness at each iteration.

Four-node shell element is used to model the steel beam while eight-node brick element is employed to model the adhesive layer and CFRP laminate. A 3D 8-node linear interface element is used to model the interface between the steel beam and the adhesive layer and between the adhesive layer and the CFRP laminate. Models with different mesh sizes were analysed in order to test the mesh sensitivity and the convergence rate and to achieve acceptable accuracy of the numerical solution.

All modelled beams are simply supported. Two stiffener plates are attached to the bottom and top flanges of the steel beam to avoid stress concentration at loading points and at the support locations. Static load is applied following an automatic load control scheme. The symmetry of the beam is employed, thus only one-half of the simulated beam is modelled to minimize the analysis processing time.

### 3.2 *Material Modelling*

The steel beam is modelled as a classical elastic plastic material with strain hardening. A bilinear stress–strain relationship is used for the steel sections in both the compression and tension behaviour. The stress–

strain relation of the CFRP laminate and adhesive material is linear up to failure. The interface between the CFRP and the adhesive is modelled using cohesive material (referred to as the Cohesive Zone Model – CZM) which is defined using three constants: maximum separation stress, value at normal separation and value at shear separation. The cohesive material behaviour is assumed exponential.

### 3.3 *Mechanical Anchorage Modelling*

A full model simulating a bolted steel joint is complex and requires tremendous computational requirements since it needs to model the bolt, the hole and an interface surface linking both of them in addition to the effect of bolts pretension on the connecting plates.

Here, instead of adopting this full bolt model at the mechanical anchorage zone, a coupled node bolted joint is used to minimize the finite element model size and to reduce the number of iterations required to obtain the solution. However, the proposed model still accounts for the prestressing effect and the friction between the steel and the CFRP laminate.

The coupling mechanism applies constraints on the degrees of freedom between the nodes that forms the two contact surfaces. In using this technique, the actual bolt was not modelled, the nodes corresponding to bolt head, nut and shaft are connected using coupling of the degree of freedom (Figure 3). Applying the coupling constraints forces the predefined nodes to move in the target nodal location so that the structural behaviour will be affected by the bolt's pretension force.

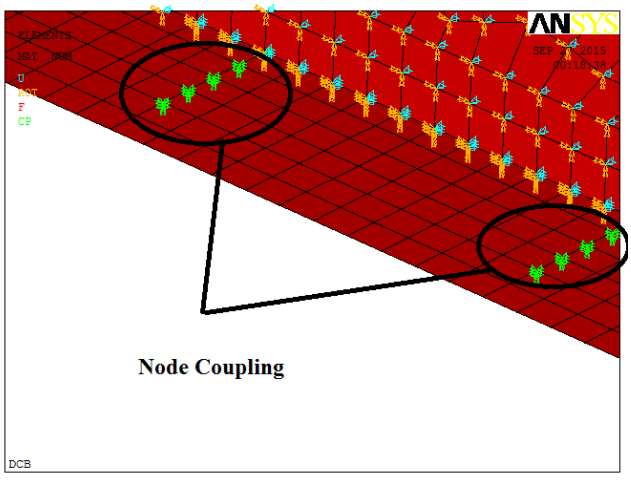


Figure 3. Bolt modelling using node coupling.

### 3.4 *The Prestressing Force*

Many techniques can be used to apply the prestressing force. In the current model, the prestressing force was modelled via applying a constant stress to the elements simulating the CFRP laminates. This stress matches the effect resulted from applying the actual prestressing force to the laminate.

## 4 NUMERICAL MODEL VERIFICATION

The present numerical analysis is executed on two stages. The first stage is concerned with the validation of the proposed numerical model results, while in the second stage the model is used to investigate the effect of prestressing level on the behaviour of the strengthened beams.

In this section, the outcomes of the first stage are outlined. Four beams of those tested in the experimental investigation [15] are simulated using proposed finite element model; these beams are CB1, CB2, B3 and B4 which are listed in Table 1.

### 4.1 *Failure Load and Load-Deflection Behaviour*

The predicted load-deflection behaviour for the control beam CB1 is compared to that of the corresponding experimental data in Figure 4. The deflection was measured experimentally at the mid-span as (shown in Figure 2). The model deflection was also recorded numerically at the same location.

It is evident from Figure 4 that the initial stiffness of the control beam predicted by the numerical model is identical to the one observed experimentally. The yield load obtained via the numerical model is 172 kN, at a corresponding deflection of 19 mm. On the other hand, the yield load observed experimentally was 172 kN at a corresponding deflection 21 mm showing good agreement between the numerical model results and the experimental programme outcomes.

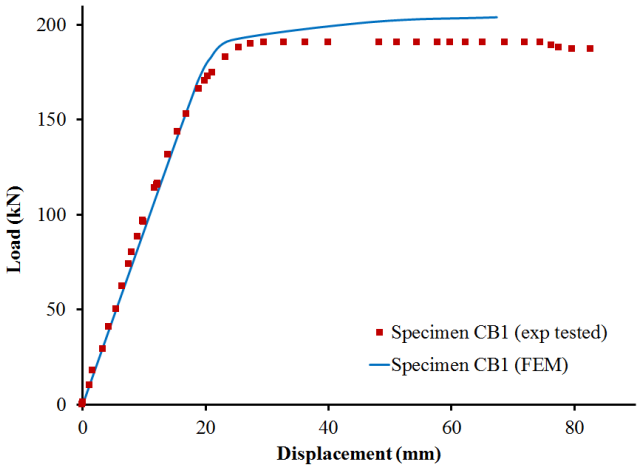


Figure 4. Load-deflection behaviour of the control beam CB1 versus the finite element analysis results of the beam's model (deflection is recorded at mid-span of the beam).

The load-deflection behaviour of the CFRP strengthened beam CB2 obtained numerically using the CZM technique versus the corresponding experimentally recorded data is shown in Figure 5. The figure reveals that the initial stiffness as well as the yield load of Beam CB2 numerically predicted are almost

identical to those measured experimentally. The ultimate load obtained using the finite element analysis is 196.8 kN, which corresponds to a premature debonding failure, at a mid-span vertical deflection of 37.7 mm. The ultimate load observed experimentally just before debonding of the CFRP laminate was 193.2 kN at corresponding deflection 30.88 mm. Once again, a good match between the experimental and numerical investigation is achieved.

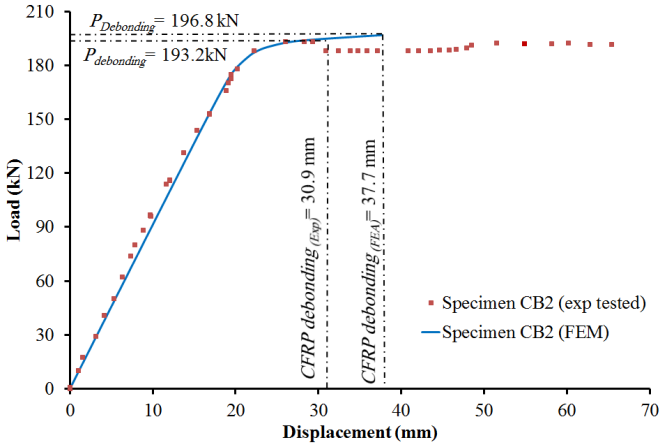


Figure 5. Load-deflection behaviour of Beam CB2 versus the finite element analysis results of the beam's model (deflection is recorded at mid-span of the beam).

Figure 6 shows the same load-deflection behaviour for the strengthened beam (Beam B3). The initial stiffness as well as the yield load of the beam numerically predicted are also very similar to those experimentally recorded. The ultimate load obtained using the finite element model is 219.2 kN at a corresponding mid-span deflection of 49.6 mm. The numerical analysis shows that the debonding load for this beam is 199.7 kN at a corresponding mid-span deflection of 38.8 mm. On the other hand, the ultimate load measured experimentally just before the CFRP laminate rupture was 204.3 kN at a corresponding deflection of 34.98. Load dropped to 199.7 kN after partial rupture of the CFRP at a corresponding mid-span deflection of 39 mm. A reasonable agreement between the numerical and experimental analysis is evident from these results.

Figure 7 shows the last of these comparisons for Beam B4. The initial stiffness of the beam numerically predicted is not as similar to the one observed experimentally as noted for the previous three beams. The finite element model shows initially stiffer behaviour compared to that of the tested beam; this is attributed to the slight imperfection of the test conditions at the time of execution and to the non-ideal behaviour of the roller/pin supports applied at both ends of the steel beam. Failure occurs by CFRP rupture in both the numerical and the experimental investigations. The ultimate numerically obtained is 196.8 kN at a corresponding mid-span deflection of 56.4 mm. Debonding of the CFRP laminated occurred at a load of 193.6 kN with a corresponding mid-span deflection of 43.6 mm. The experimental programme revealed a load just before the CFRP laminate debonding of 182.7 kN at a corresponding mid-span deflection 38.46 mm. Furthermore, the failure load recorded experimentally for this specimen was 195.3 kN at a corresponding mid-span deflection of 74.4 mm. Once again, a reasonable agreement between the experimental and numerical results is shown.

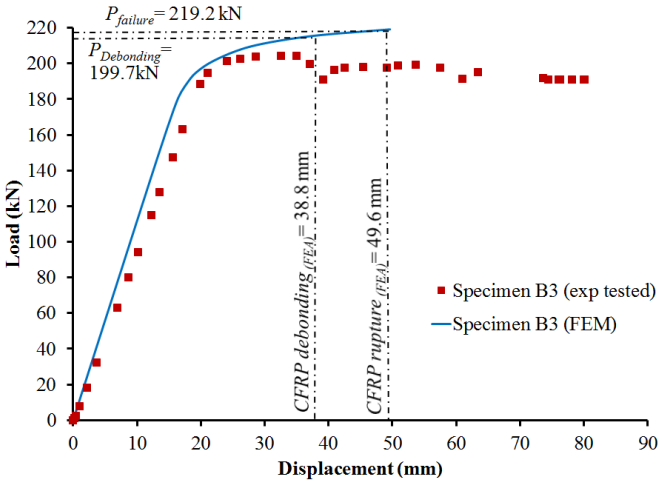


Figure 6. Load-deflection behaviour of Beam B3 versus the finite element analysis results of the beam's model (deflection is recorded at mid-span of the beam).

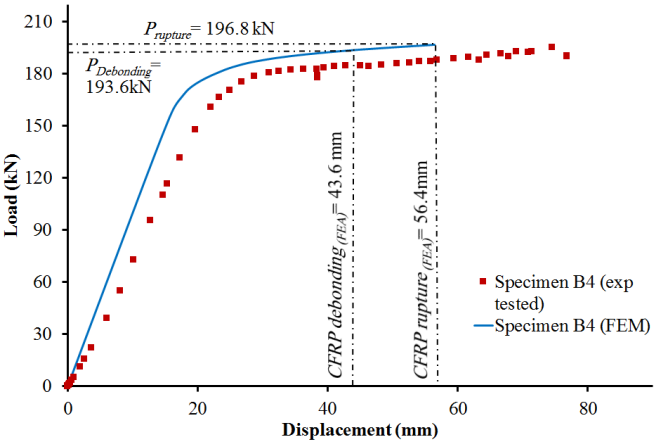


Figure 7. Load-deflection behaviour of Beam B4 versus the finite element analysis results of the beam's model (deflection is recorded at mid-span of the beam).

Table 6 summarizes the value of the failure load recorded experimentally and obtained using the numerical model. It is evident form this table that the maximum discrepancy between both loads for all the analysed beams is about 7%.

## 4.2 *Failure Modes*

Figure 8 shows the deformed shape of Beam CB2. The figure reveals a good agreement between the numerical analysis results and the observed premature failure mode of the experimental investigation. The

debonding took place at both ends of the CFRP laminate and it was almost pure mode-I.

Table 6. Failure loads obtained numerically and experimentally for the analysed beams.

| Beam | Failure load | | |
|---|---|---|---|
| | Num. (kN) | Exp (kN) | Exp./Num |
| CB1 | 172 | 172 | 0 |
| CB2 | 196.8 | 193.2 | 98.2% |
| B3-25-AN | 219.2 | 204.3 | 93.2% |
| B4-45-AN | 196.8 | 195.3 | 99.2% |

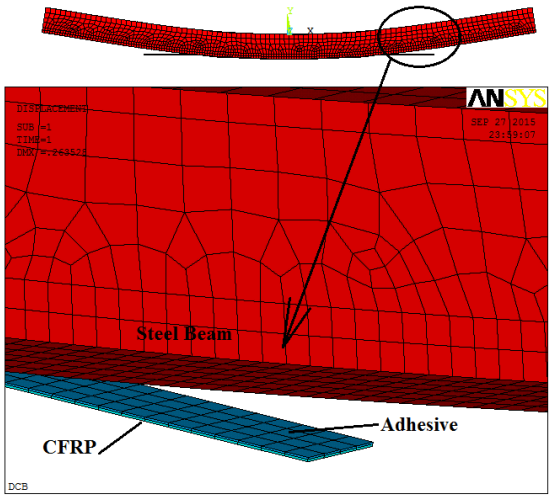


Figure 8. Numerically recorded deformed shape and CFRP debonding of Beam CB2.

Figure 9 shows the typical deformed shape of Beams B3 and Beam B4. It shows the effect of adding the mechanical anchorage on the premature debonding failure, which took place at mid span of the CFRP laminate instead the previously observed end debonding of Beam CB1. The debonding failure is in agreement of the experimental observation. The failure took the form of mixed mode-II where a combination of slippage and shear rupture took place in the adhesive layer.

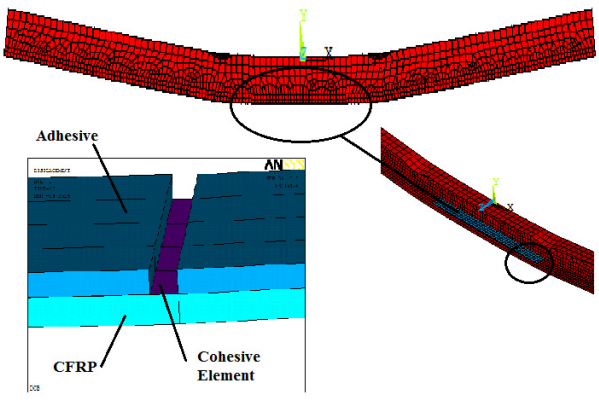


Figure 9. Numerically recorded deformed shape and CFRP debonding of Beam B3.

Figure 10 shows the stress on the cohesive zone right before and after debonding. The energy release mechanism can be clearly observed through the presented figure.

At the early stage of loading, the stress distribution is almost constant on the cohesive elements. The release of energy started gradually from the middle and extended towards both ends of the zone. Right before the failure. Finally, after debonding, all the energy has released and the stress distribution on the cohesive zone become very small value and approaches zero. The debonding mode in this case is considered as mixed mode II: in this mode, the separation plan is affected by both normal and shear stress and therefore, the distortion observed in the cohesive zone and the adhesive layer is in two directions. The slippage between the two surfaces lead to a complete separation between the adhesive layer and the cohesive zone and another separation among the adhesive layer.

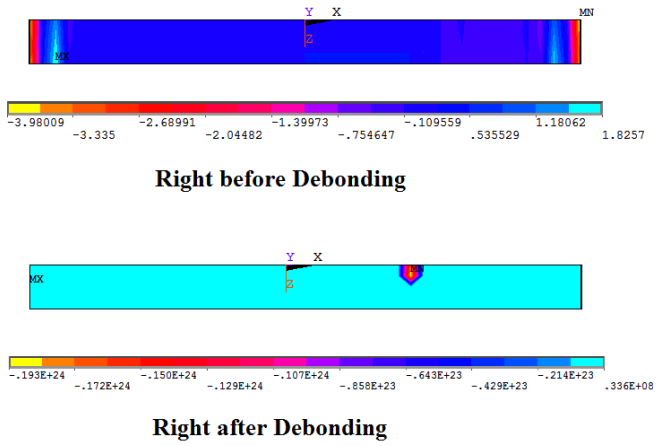


Figure 10. Shear stress distribution right before and after CFRP laminate debonding. (N.B. Lower figure reveals only shear stress distribution as these unrealistic stress values are obtained from non-converged iteration).

## 5 LAMINATE PRESTRESSING EFFECT

At this stage of analysis, the validated finite element model is used to evaluate the effect of increasing the prestressing level applied to the CFRP laminate.

Three beams are analysed at this stage: Beam B3-15%, Beam B3-40% and Beam B3-70%. The three beams have the same configuration and material properties of beam B3 introduced at the first stage but with prestressing force of 15%, 40% and 70% of the CFRP laminate's tensile strength, respectively. As such, the three beams have prestressing forces of 55.8 kN, 140.8 kN and 260.4 kN, respectively. The three beams are analysed and the results are compared to the behaviour of Beam B3 previously tested and numerically modelled for which the CFRP laminate was prestressed using a prestressing force of 25 kN: this level of prestressing corresponds to 7% of the CFRP tensile strength.

A comparison between the values of the yield and the ultimate loads for each beam is shown in Table 7. The table also shows the mode of failure for corresponding to each prestressing level. Furthermore, the load versus the mid-span deflections for the beams are plotted in Figure 11.

It is evident from Figure 11 that the load-deflection behaviour of theses beams, which have different prestressing levels, is similar. However, it is noticed that increasing the laminate prestressing level increases the yield load (Table 7) and the overall section stiffness (Figure 11). The results show a slight increase in the yield strength of the strengthened section but with no significant difference between the 7%, 15% and the 40% prestressing levels where the loads initiating yielding were found to be 193.6 kN, 196.8kN and 200 kN for the above mentioned three levels of prestressing, respectively. However, the results reveal that the ultimate load of the 40% prestress level case is significantly higher than strengthened beams with lower prestressing levels. Thus, it is concluded that increasing the prestressing level increases the ultimate load capacity up to a certain limiting value.

Increasing the prestressing load up to 70% enhances the section overall stiffness but the failure mode changes from debonding to CFRP laminate rupture at a very early stage of loading. The early rupture failure of the CFRP laminate is attributed to the high values of initial stress generated in the laminate due to the high level of prestressing; thus, the laminate cannot accommodate more stresses during loading phase leading to a lower value for the overall capacity of the strengthened beam. Therefore, it is recommended not to increase the prestressing level above 40% of the laminate tensile capacity.

Table 7. Failure loads of Beam B3 for different prestressing.

| Beam no. | B3-7% | B3-15% | B3-40% | B3-70% |
|---|---|---|---|---|
| Yield load (kN) | 193.6 | 196.8 | 200 | N/A |
| Ultimate load (kN) | 216 | 219.2 | 240 | 135.2 |
| Mode of failure | CFRP Debonding | CFRP Debonding | CFRP Debonding | CFRP Rupture |

Figures 12 and 13 show the variation of shear and normal stresses along the CFRP strip at a load level of 100 kN. It is observed that the normal stress sharply reduced along the strip length when increasing the prestressing force from 7% to 40%. The stress peak point shifted from under the concentrated load to the end side of the CFRP laminate. However, the stresses at the end of the CFRP laminate remain at the same value. Furthermore, the shear stress decreased through the shear span until it reached zero in the constant moment zone for the both prestressing levels.

This is attributed to the fact that the prestressing force contributes in supporting the concentrated loads at the middle of the span. Increasing the prestressing level from 7% to 40% adds enhance this support and reduces the peak point of the stress as shown both Figures 12 and 13.

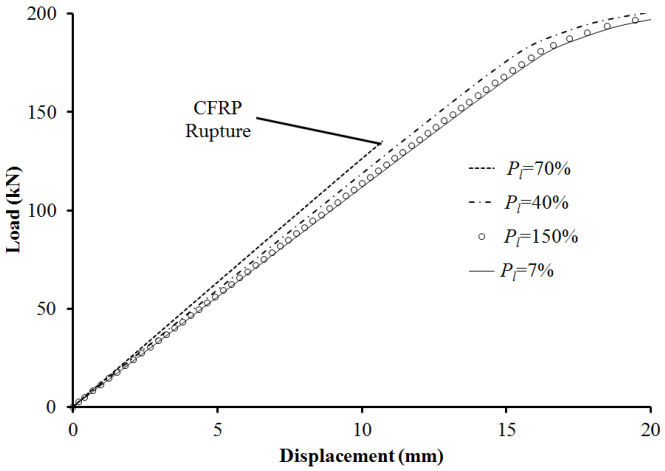


Figure 11. Load-deflection behaviour for beam B3 at different prestressing levels of the CFRP laminate.

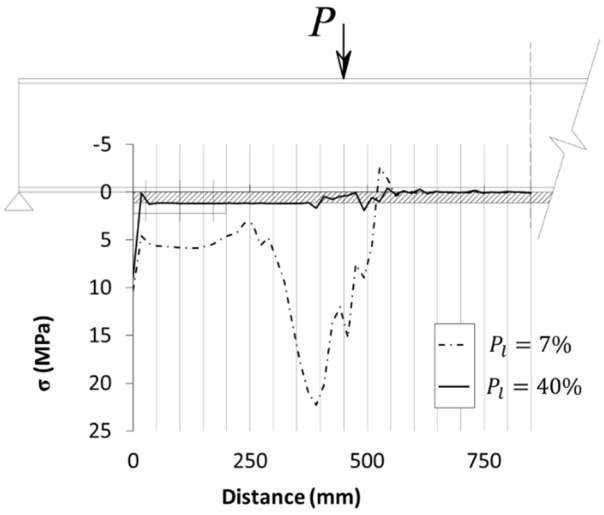


Figure 12. Normal stress for Beam B3 at CFRP laminate prestressing levels of 7% and 40% (P=100 kN).

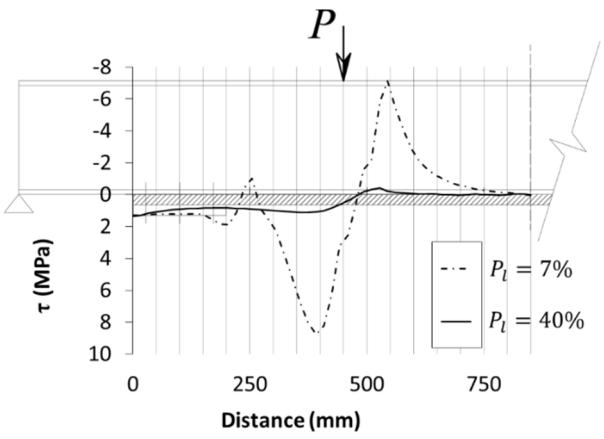


Figure 13. Shear stress for Beam B3 at CFRP laminate prestressing levels of 7% and 40% (P=100 kN).

## 6 CONCLUSIONS

An experimental programme was previously conducted to investigate the flexural behaviour of steel beams strengthened with prestressed CFRP laminate having mechanical end anchorage system. In this paper, a numerical model was developed and its results was verified against the results of the previously executed experimental programme. The model results agree well with the experimental results with a variation of less than 8% in the values of the ultimate loads.

The proposed numerical model considers both the material and geometric nonlinearities as well as the debonding between the CFRP laminate system and the steel beam. The Cohesive Zone Model (CZM) technique was adopted to model the CFRP laminate debonding from the steel beam and proved to be effective and accurate technique.

Based on the numerical analysis results, it is concluded that CFRP prestressing increases the ultimate load of the CFRP strengthened steel beam. The said prestressing also delayed the premature debonding failure of the CFRP laminate from the steel beam.

The numerical analysis reveals that increasing the prestressing force in the CFRP laminate enhances the characteristics of the steel-CFRP hybrid section in terms of load capacity and bond strength. However, increasing the prestressing force to a high level (e.g. 70% of the CFRP laminate tensile strength) causes the laminate to rupture prematurely which significantly decrease the section capacity. Thus, it is recommended to use a level of prestressing which does not exceed 40% of the CFRP laminate tensile capacity. However, it is recommended to extend the scope of the current study in order to include different beam sizes to verify this conclusion. Then, the optimum prestressing level can be linked to the ratio between the area of the steel beam to the area of the CFRP laminate and also to the grade of the steel material.

## 7 ACKNOWLEDGMENTS

The authors would like to acknowledge the contribution of King Abdulaziz University for facilitating the experimental programme in their laboratory.

## 8 PREFERENCES

[1] Linghoff, D., Al-Emrani, M., Kliger, R. 2010. Performance of steel beams strengthened with CFRP laminate–Part 1: laboratory tests. Composites Part B: Engineering, 41(7):509-515.

[2] Linghoff, D., Al-Emrani, M. , Kliger, R. 2010. Performance of steel beams strengthened with CFRP laminate–Part 2: FE analyses. Composites Part B: Engineering, 41(7):516-522.

[3] Sayed-Ahmed, E.Y. 2006. Numerical Investigation into Strengthening Steel I-Section Beams Using CFRP Strips. Proceedings, Structures Congress, ASCE, St. Louis, USA, 18-20 May 2006.

[4] Sayed-Ahmed, E.Y. 2004. Strengthening of Thin-Walled Steel I-Section Beams Using CFRP Strips. Proceedings, 4th International Conference on Advanced Composite Materials in Bridges and Structures (ACMBS IV), Calgary, Alberta, Canada.

[5] Bakay, R., Sayed-Ahmed, E.Y., Shrive, N.G. 2009. Interfacial debonding failure for reinforced concrete beams strengthened with carbon-fibre-reinforced polymer strips. Canadian Journal of Civil Engineering, 36(1):103-121.

[6] Hosny, A., Sayed-Ahmed, E.Y., Abdelrahman, A.A., Alhlaby, N.A. 2006. Strengthening precast-prestressed hollow core slabs to resist negative moments using carbon fibre reinforced polymer strips: an experimental investigation and a critical review of Canadian Standards Association S806-02. Canadian Journal of Civil Engineering, 33(8):955-967.

[7] Meier, U. 1995. Strengthening of structures using carbon fibre/epoxy composites. Construction and Building Materials, 9(6):341-351.

[8] Sayed-Ahmed, E.Y., Riad, A.H., Shrive, N.G. 2004. Flexural strengthening of precast reinforced concrete bridge girders using bonded carbon fibre reinforced polymer strips or external post-tensioning. Canadian Journal of Civil Engineering, 31(3):499-512.

[9] Sayed-Ahmed, E.Y., Lissel, S.L., Tadros, G. and, Shrive, N.G. 1999. Carbon Fibre Reinforced Polymers (CFRP) Post-Tensioned Masonry Diaphragm Walls: Prestressing, Behaviour and Design Recommendations. Canadian Journal of Civil Engineering, 26(3): pp. 324-344.

[10] Abdelrazki, A. T., Elserwi, A.A., Sayed-Ahmed, E.Y. 2016. Steel Columns Strengthened with Prestressed FRP Laminate. Proceeding 2nd International Conference on Infrastructure Management, Assessment and Rehabilitation Techniques ICIMART'16, American University in Sharjah, UAE, March 8-10.

[11] Lenwari, Akhrawat, Thaksin Thepchatri, and Pedro Albrecht. "Debonding strength of steel beams strengthened with CFRP plates." Journal of Composites for Construction 10.1 (2006): 69-78.

[12] Buyukozturk, Oral, Oguz Gunes, and Erdem Karaca. "Progress on understanding debonding problems in reinforced concrete and steel members strengthened using FRP composites." Construction and Building Materials 18.1 (2004): 9-19.

[13] Zhao, Xiao-Ling, and Lei Zhang. "State-of-the-art review on FRP strengthened steel structures." Engineering Structures 29.8 (2007): 1808-1823.

[14] You, Y.C., Choi, K.S., Kim J. 2012. An experimental investigation on flexural behavior of RC beams strengthened with pre-stressed CFRP strips using a durable anchorage system. Composites Part B: Engineering 2012, 43(8):3026-3036.

[15] Gharib, M.A., Khushefati, W.H., Khedr, M.A., Sayed-Ahmed, E.Y. 2015. Performance of steel beams strengthened with prestressed CFRP laminate. Electronic Journal of Structural Engineering, 15: 60-69.

[16] You, Y., Choi, K., Kim, J. 2012. An experimental investigation on flexural behavior of RC beams strengthened with prestressed CFRP strips using a durable anchorage system. Composites Part B: Engineering, 43(8): 3026–3036.

[17] Colombi, P., Poggi, C. 2006. An experimental, analytical and numerical study of the static behavior of steel beams reinforced by pultruded CFRP strips. Composites Part B: Engineering, 37(1): 64–73.

[18] Al-Emrani, M., Kliger, R. 2006. Experimental and numerical investigation of the behaviour and strength of composite

steel-CFRP members. Advances in Structural Engineering, 9(6): 819-831.
[19] Al-Zubaidya, H., Al-Mahaidib, R., Zhaoa, X. 2012. Experimental investigation of bond characteristics between CFRP fabrics and steel plate joints under impact tensile loads Composite Structures, 94(2): 510–518.
[20] Jones, S. and Civjan, S. 2003. Application of Fiber Reinforced Polymer Overlays to Extend Steel Fatigue Life. Journal of Composites for Construction, ASCE, 7(4): 331-338.
[21] Narmashiri, K., Jumaat, M.Z., Sulong, N.R. 2010. Investigation on end anchoring of CFRP strengthened steel I-beams. Inter-national Journal of the Physical Sciences, 5(9):1360-1371.
[22] Narmashiri, K., Sulong, N.R., Jumaat, M.Z. 2012. Failure analysis and structural behaviour of CFRP strengthened steel I-beams. Construction and building materials, 30:1-9.
[23] Ghareeb, M.A., Khedr, M.A., Sayed-Ahmed, E.Y. 2013. CFRP Strengthening of Steel I-Beam against Local Web Buck-ling: a Numerical Analysis. Research and Applications in Structural Engineering, Mechanics & Computation: Proceedings of the Fifth International Conference on Structural Engineering, Mechanics & Computation, A. Zingoni (ed.), Taylor & Francis Group Ltd, Cape Town, South Africa, 2-4 Sept.
[24] Seleem, M., Sharaky, I., Sallam, H. 2010. Flexural behavior of steel beams strengthened by carbon fiber reinforced polymer plates–Three dimensional finite element simulation. Materials and& Design, 31(3):1317-1324.
[25] Mergheim, J., Kuhl, E., Steinmann, P. 2005. A finite element method for the computational modelling of cohesive cracks. International Journal for Numerical Methods in Engineering, 63(2): 276-289.
[26] Fawzia, S., Al-Mahaidi, R., Zhao, X. 2006. Experimental and finite element analysis of a double strap joint between steel plates and normal modulus CFRP. Composite structures, 75(1):156-162.
[27] De Lorenzis, L., Zavarise, G. 2009. Cohesive zone modelling of interfacial stresses in plated beams. International Journal of Solids and Structures 46(24):4181-4191.
[28] Barbero, E.J. 2013. Finite Element Analysis of Composite Materials Using ANSYS®. CRC Press.